

Saturable absorption and self-focusing properties of Molybdenum Diselenide thin films

Zahra Dehghani ^{*1}, Iman Sahraneshin Bazzi¹, Davoud Vahedi Fakhrabad¹, Fatemeh Ostovari²

¹ Department of Physics, University of Neyshabur, Neyshabur, Iran

² Department of Physics, Faculty of Science, Yazd University, Yazd, Iran

Received 14 January 2023,

revised 29 April 2023,

accepted 17 May 2023,

available online 22 May 2023

Abstract

The next generation of photonics and nano-optical devices may be based on two-dimensional (2D) transition metal dichalcogenides (TMDs). In this research, molybdenum diselenide (MoSe₂) nanosheets, as one important member of TMDs, have been synthesized by the solvothermal method and characterized through XRD patterns, SEM, and TEM images. Nanosheets were found to have a hexagonal phase based on XRD patterns and the crystallinity percentage is 24.8%. The lattice constants of the hexagonal phase of MoSe₂ are calculated as $a = 3.08 \text{ \AA}$, $c = 13.72 \text{ \AA}$. The calculated average value of the crystallite size, dislocation density, and micro strain are 21.935 nm, $2.138 \times 10^{-4} \text{ nm}^{-2}$ and 9.070, respectively. A few layers of nanosheets without wrinkles were observed on TEM and SEM. Next, the synthesized nanosheets were employed to prepare thin films with three different thicknesses using the spin coating method. By employing a continuous wave (CW) Nd:YAG laser at 532 nm via a Z-scan approach, this study investigates how thin film thickness affects the thermal nonlinear optical (NLO) responses of MoSe₂ nanosheets. The magnitude of NLO coefficients of the prepared thin films decreased with increasing film thickness. It is observed that the prepared thin films possess saturable absorption (SA) as well as the self-focusing effect. Saturable absorbers and mode-locking devices can be developed with thin films because of their improved NLO properties.

Keywords: Nonlinear Optics; Saturable Absorption; Self-focusing; Thin Film.

How to cite this article

Dehghani Z., Sahraneshin Bazzi I., Vahedi Fakhrabad D., Ostovari F., Saturable absorption and self-focusing properties of Molybdenum Diselenide thin films. *Int. J. Nano Dimens.*, 2023; 14(3): 257-266.

INTRODUCTION

The prepared thin films of semiconductor materials are having possible use in computers, drugs and dye-sensitized solar cell devices. The recent innovations in field of thin film technology have been attracted to many researchers and industries and makes it major field of research and development recently [1]. Due to the fact that transition metal dichalcogenides (TMDs) exhibit a thickness dependence optical property, they have gained considerable attention as two-dimensional (2D) semiconductors. As materials change from bulk to single layer, TMDs transition from indirect bandgaps to direct bandgaps, allowing bandgap engineering. High carrier mobility and outstanding nonlinear optical (NLO) absorption are two of the

benefits of this novel feature [2].

It has been experimentally demonstrated that molybdenum diselenide (MoSe₂), as one of the most important TMDs, exhibits promising NLO properties over a wide range of spectral ranges, including giant two-photon absorption, saturable absorption, strong nonlinear self-focusing, and nonlinear intensity dependent absorption and scattering, leading to optical limiting [3, 4]. In addition, MoSe₂ was reported to have stronger saturable absorption (SA) than graphene at the wavelength of 800 nm with an imaginary part of third-order NLO susceptibility of $-1.56 \times 10^{-14} \text{ esu}$ [5]. In Ref. [6], the main study is to investigate the optical properties of purchased MoSe₂ nanosheets, which had SA and self-focusing phenomena. The nonlinear refractive indices were in the range

* Corresponding Author Email: zahra.dehghani@neyshabur.ac.ir; z_dehghani2004@yahoo.com

Copyright © 2023 The Authors.



This work is licensed under a Creative Commons Attribution-NonCommercial 4.0 International License.,

To view a copy of this license, visit <https://creativecommons.org/licenses/by-nc/4.0/>

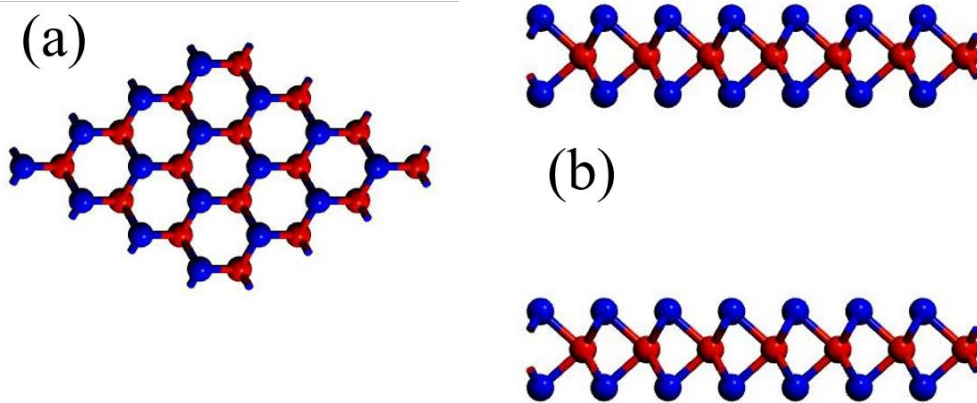


Fig. 1. Schematic of structure of monolayer (a) top view and, (b) side view.

of $10^{-7} \text{ cm}^2/W$ and the nonlinear absorption coefficients were in order of $10^{-3} \text{ cm}/W$

In photonic and optoelectronic devices, NLO property plays an important role in improving their performance via the interaction between light and matter [7]. A variety of experiments are conducted to estimate NLO properties, including nonlinear interferometry, degenerate four wave mixing, nearly degenerate three wave mixing, beam distortion measurement, and moiré reflectometry [8]. Despite its simplicity and sensitivity, the Z-scan is an excellent method to calculate nonlinear coefficients both in magnitude and sign [9].

In many works, NLO properties have been investigated, but as far as we know, in majority of these works, the experiment was done with the help of different pulsed lasers [10-18]. Indeed, The NLO properties have been demonstrated to be dependent on the laser type (pulsed or CW), pulse width, and repetition rate [19, 20]. In addition, there is some considerable work is reported on the various properties of MoSe_2 thin films [21-24]. However, despite the interest aroused by NLO properties, a systematic study of the thickness dependent NLO and Z-scan studies on these films by a CW laser is lacking.

Given this, in present work, we have fabricated the thin films of MoSe_2 of different thicknesses by spin coating technique and aim to investigate NLO responses of MoSe_2 thin films with various thicknesses using the Z-scan technique in CW regime.

MATERIALS AND METHODS

Synthesis of MoSe_2 nanosheets

High purity Se powder and Sodium molybdate

$\text{Na}_2\text{MoO}_4 \cdot \text{H}_2\text{O}$ and Ammonium para molybdate $(\text{NH}_4)_2\text{MoO}_4 \cdot 2\text{H}_2\text{O}$ were used for the synthesis of MoSe_2 by Solvothermal chemical root method. All chemicals and solvents used for synthesis of MoSe_2 nanosheets were purchased from commercial suppliers (Aldrich or Merck) and used as received. In a typical procedure, 0.479 g of $\text{Na}_2\text{MoO}_4 \cdot \text{H}_2\text{O}$ and 0.316 g of Se powder was employed for molybdenum source for preparing samples. First, precursor materials were added to 10 ml Hydrazine monohydrate and 60 ml deionized water, which was stirred magnetically until a red color was obtained. Next, by adding 1M sodium hydroxide solution, the pH of the solution is adjusted to pH 12. A Teflon-lined autoclave (110 mL) is used to sterilize the solution after stirring for 30 minutes. We sealed and maintained the autoclave at 200°C for 48 hours before allowing it to naturally cool to room temperature. We collected a black product through centrifugation, washed several times with deionized water and absolute ethanol, and finally vacuum-dried for 12 hours, resulting in a black powder [25, 26]. Schematic of structure of MoSe_2 monolayer illustrate in Fig. 1.

Preparation of MoSe_2 Thin Films

Before the coating process, the glass substrates were cleaned with soap water, methanol then dried carefully to remove impurities present on the substrates [23, 27]. The MoSe_2 thin film was deposited on the Si/SiO₂ substrate was achieved by spin-coating as the following procedure. First, we prepare the solution of dispersed nanosheets in DMF. As shown in Fig. 2, 5000 rpm spin coating and 100°C annealing were used to deposit the solution. Then, under heating inside a vacuum

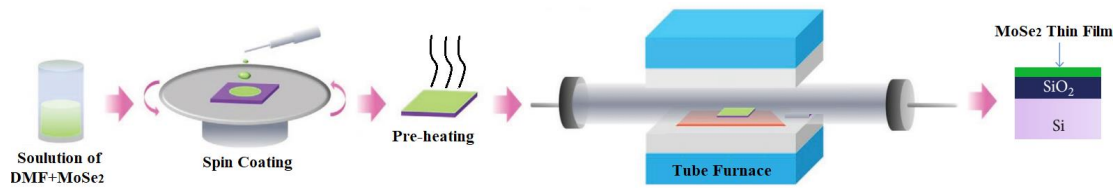


Fig. 2. Procedure of spin coating for preparing thin film.

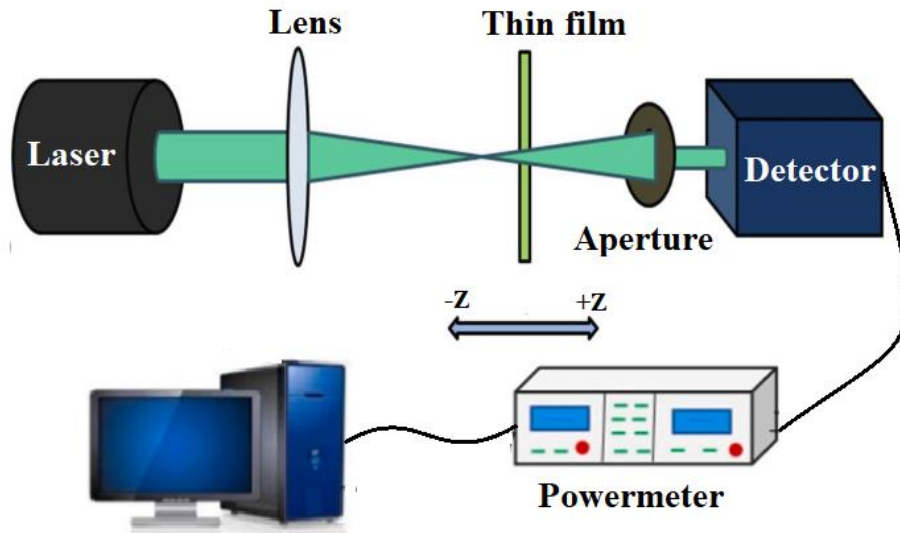


Fig. 3. The schematic Z-scan experiment setup.

oven at 70 °C (10 h), MoSe₂ was formed as can be observed by changing the color of the thin film [22]. Finally, the coated substrate was placed at the center of a tube furnace (Fig. 2) at ambient atmosphere [23].

The obtained thin film with one spin coating has the smallest thickness, which will be denoted by S1. To have higher thicknesses, we repeat the number of spin coating. By repeating the spin coating for the second time, we will have sample S2, and by repeating the spin coating for the third time, sample S3 will be obtained. So, we have three samples with different thicknesses, which we name as S1, S2, and S3.

Z-scan theory

To measure the NLO coefficients including refractive and absorption indices of the prepared thin films, the Z-scan method was employed. The experimental setup is schematically depicted in Fig. 3. There was a CW neodymium-doped yttrium aluminum garnet (Nd : YAG) laser at 532 nm used as the light source. The laser beam was focused

through the plano-convex lens to obtain the beam waist (ω_0) of around 42 μm at the position of $z = 0$. The power of laser was 50 mW for all samples. During the axial movement of the prepared sample, using a digital power meter with a closed aperture, the far field transmittance intensity varied [28]. Thus, it is possible to determine the nonlinear refractive coefficient of a material using the far field energy density of a beam [29].

A NLO property of materials is saturable absorption (SA) under high intensity light, such as a laser beam. In the NLO material, incident photons absorb electrons in the valence band and are excited into the conduction band when they interact with the material. As shown in Fig. 4a [4], at low incident intensity most of the photons are absorbed and this therefore results in low transmission. In contrast, for relatively high incident laser beam intensities, a large number of electrons is excited to fill the conduction band of a SA sample whose cross-section of the ground state is smaller than that of excited states, and the conduction band cannot accept any more

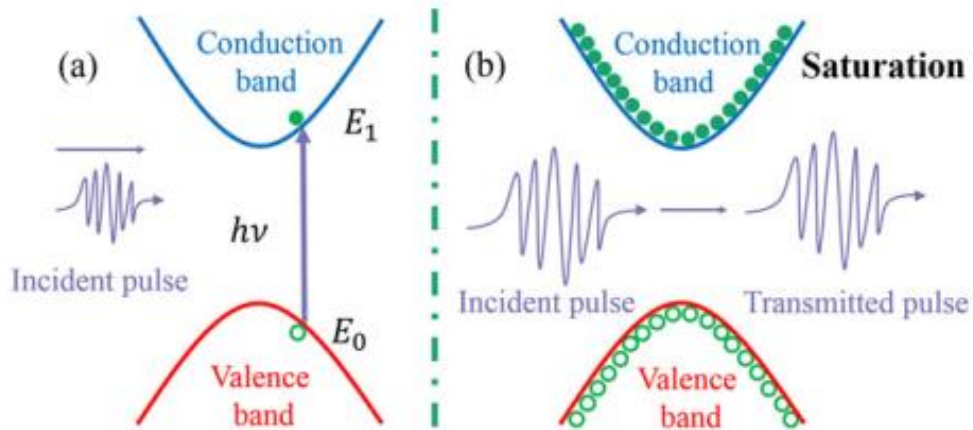


Fig. 4. The principle of SA due to the Pauli-blocking. (a) A low-intensity incident laser beam passes through a NLO material with a low transmission, (b) while the high intensity one results in high transmission.

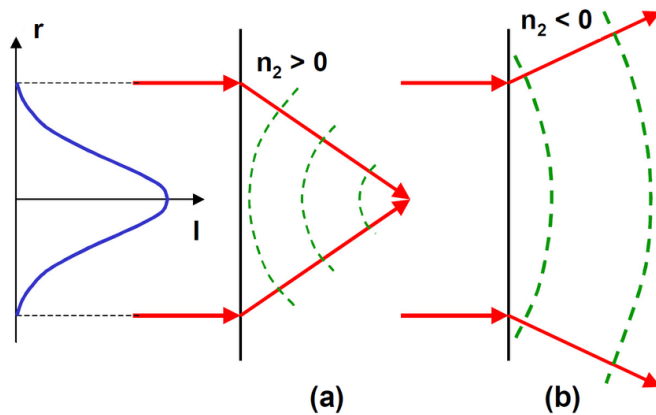


Fig. 5. (a) Self-focusing and, (b) self-defocusing of a Gaussian beam.

incoming electrons. Consequently, most of the incident photons are not absorbed and transverse the material, that is, high transmission, as seen in Fig. 4b [4].

Hence, the SA behavior of materials can be studied by Z-scan or I-scan techniques via the measurement of the transmitted light as a function of the incident light [4].

It is noteworthy, however, that one of the main self-action effects in laser-material interactions is self-focusing. The laser beams are able to modify their front medium by using nonlinear responses of material in this way, allowing them to propagate more suitable. Here, one can express the refractive index of the material as $n = n_0 + n_2 I(r)$ in which n_0 refers to linear refraction, n_2 denotes nonlinear refraction index, and $I(r)$ determine the beam intensity distribution along the radial coordinator

[30]. Therefore, the wave front of the beam becomes increasingly distorted as it propagates through the medium, as shown in Fig. 5a [31]. It appears that the beam is focused on its own since the optical rays always propagate perpendicular to the wave front. For NLO materials with $n_2 < 0$ the wave front bends in the material as the central part propagates faster than the edges Fig. 5b, and the beam appears to suffer defocusing [31].

RESULTS AND DISCUSSIONS

Characterization of MoSe₂ nanosheets

Analyses of the MoSe₂ nanosheet structure were carried out by SEM, TEM images, and XRD pattern. Fig. 6a illustrates the SEM image and Fig. 6b depicts the TEM image of MoSe₂ nanosheet. SEM and TEM studies of MoSe₂ revealed few layers and no wrinkles [6] in the prepared nanosheets.

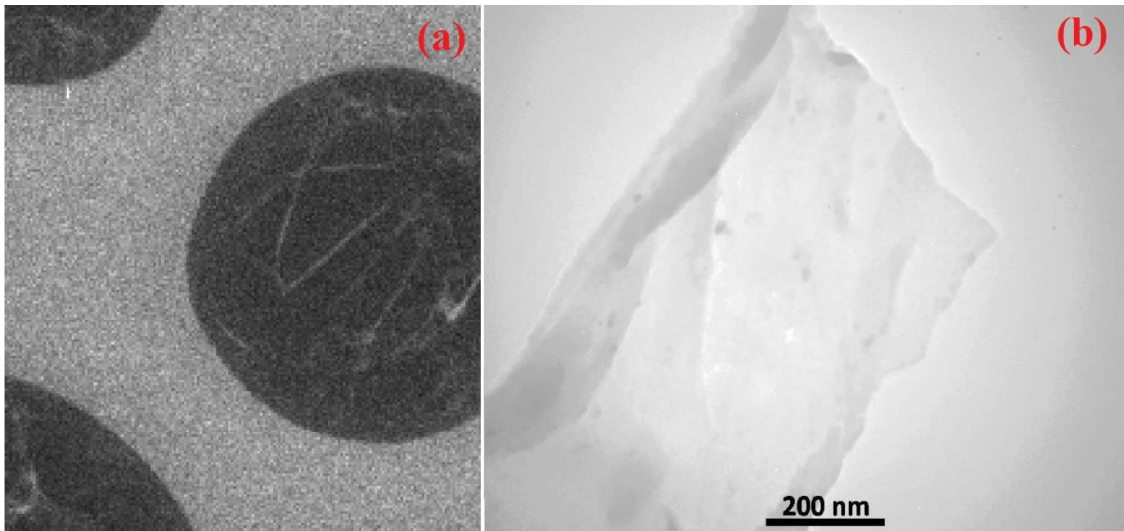


Fig. 6. a) SEM and, b) TEM analysis of the synthesized nanosheets.

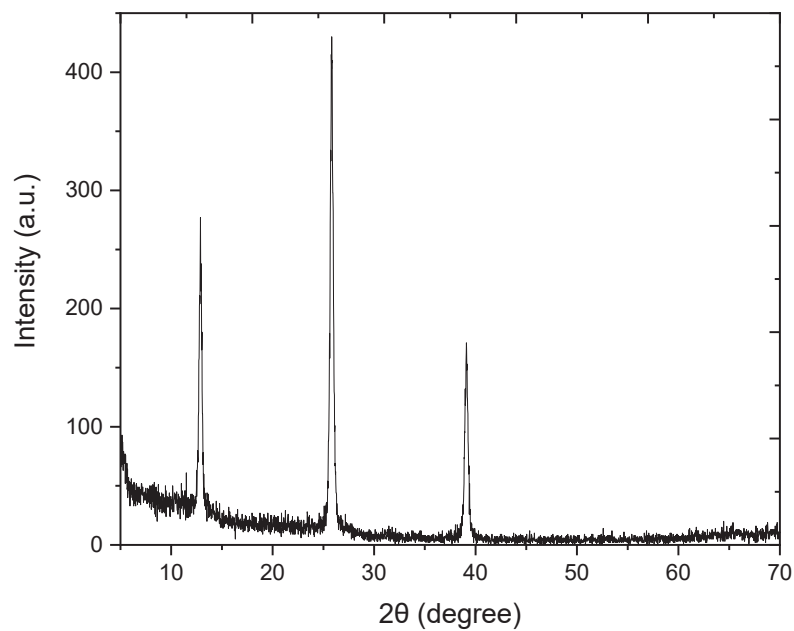


Fig. 7. XRD pattern of the synthesized nanosheets.

The diffraction peaks of typical XRD patterns for MoSe₂ nanosheets in Fig. 7 can be indexed to hexagonal phase. The Scherer formula is used to estimate the crystal size, and it is given as below [32]:

$$D = \frac{k\lambda}{\beta \cos\theta} \quad (1)$$

Where k is approximately equal to 0.94, λ is the wavelength of X-ray (1.5406 Å), β is the width of the peak at half maximum intensity and θ is the

diffraction angle.

$$d_{hkl} = \frac{\lambda}{2\sin\theta_{hkl}} \quad (2)$$

The dislocation parameter is a crystallographic defect, presents an irregularity within a crystal structure. The presence of dislocations (δ) strongly influences many of the properties of materials. We can calculate the dislocation density of our MoSe₂ sample by the relation below [33]:

$$\delta = \frac{1}{D^2} \quad (3)$$

Table 1. The structural parameters of nanosheets.

Peak No.	2θ (°)	(hkl)	β (°)	d _{hkl}	D (nm)	δ (nm ⁻²) × 10 ⁻³	ε × 10 ⁻³
1	12.887	(002)	0.409	6.864	19.525	2.623	15.819
2	25.822	(004)	0.379	3.447	21.530	2.157	7.205
3	39.102	(103)	0.341	2.302	24.749	1.633	4.185

Table 2. The lattice parameter of hexagonal phase of nanosheets.

Lattice Constant	Standard Values (°A)	Calculated Values (°A)
a	3.15	3.08
c	12.29	13.72

Where, the D is the crystallite size of our material. Furthermore, the micro strain ε in the MoSe₂ was determined using the relation [34]:

$$\epsilon = \frac{\beta}{4 \tan \theta} \tag{4}$$

The structural parameters of MoSe₂ nanosheets are given in Table 1. The calculated average value of the crystallite size, dislocation density, and micro strain are 21.935 nm; 2.138 × 10⁻³ nm⁻² and 9.070 × 10⁻³.

To determine the lattice parameter of hexagonal phase of MoSe₂ nanosheets, we can use the following equation:

$$\frac{1}{d_{hkl}^2} = \frac{4 \times (h^2 + hk + k^2)}{3a^2} + \frac{l^2}{c^2} \tag{5}$$

The obtained lattice parameters are reported in Table 2. Our calculated values are in very good approximation to standard values.

Moreover, an XRD deconvolution method can be used to determine crystallinity percentages by separating amorphous and crystalline contributions. The crystallinity can be calculated by dividing the integrated area under all XRD peaks by the integrated area of all crystalline peaks as below equation [35]:

$$\text{Crystallinity index} = \frac{\text{Area of all the crystalline peaks}}{\text{Area of all crystalline and amorphous peaks}} \tag{6}$$

Crystallinity of the synthesized MoSe₂ nanosheets is 24.8 %.

Saturable absorption process of the prepared MoSe₂ thin film

Saturable absorption is a phenomenon caused by the Pauli-blocking effect, where a transition state is fully occupied and can no longer accept incoming electrons [4]. The nonlinear absorption index of prepared MoSe₂ thin film can be calculated by employing open aperture Z-scan. The normalized transmittance T(Z) was plotted as a function of position (Z) for three different thicknesses are depicted in Fig. 8. As can be seen the transmission raises as regards position and shows a maximum at focus, which indicates the outstanding saturation absorption (SA) phenomenon and positive sign of nonlinear absorption index. The SA effect is originated in the sample due to the dominance of ground state linear absorption over the excited state absorption [27]. By fitting the experimental open aperture data with the below theoretical equation as shown in Fig. 8a, the nonlinear absorption index can be obtained using the following equation [36, 37]:

$$T(z, S = 1) = \sum_{m=0}^{\infty} \frac{(-\beta I_0 L_{eff})^m}{\left(1 + \left(\frac{z}{z_0}\right)^2\right)^m} (m + 1)^{3/2} \tag{7}$$

Herein, T(z) refers to the normalized transmittance, β denotes the nonlinear absorption coefficient, L_{eff} = (1 - e^{-αl})/α is the effective thickness of the prepared thin films, α refers to the linear absorption index at low intensity, L is the thickness of the prepared thin films, I₀ = 2P₀/πω₀² denotes the incident intensity at focal point calculated to be 1805.39 W/cm², z₀ = kω₀²/2 is



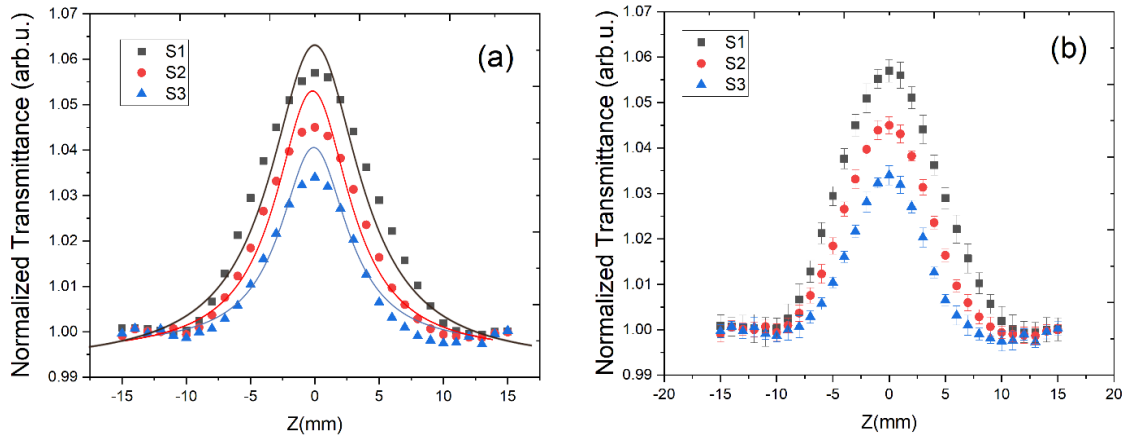


Fig. 8. Open aperture curves of different thicknesses of the prepared thin film by a) fitting the experimental data with the theory and, b) taking into account the error bar.

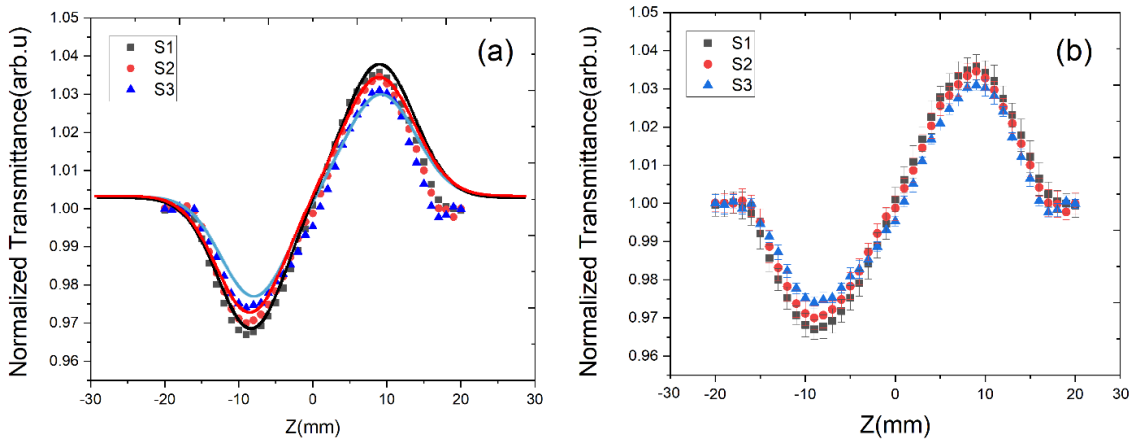


Fig. 9. Pure closed-aperture curves of different thicknesses of the prepared thin film by a) fitting the experimental data with the theory and, b) taking into account the error bar.

the Rayleigh length obtained about 10.42 mm and z is the position of the prepared thin films. Fig. 8b illustrates the experimental data with taking into account the error bar by repeating the performing of the experiment for five times.

Self-focusing analysis the prepared MoSe_2 thin film

Self-focusing is a NLO process induced by the change in refractive index of materials exposed to intense electromagnetic radiation. The closed-aperture transmittance curves of different thickness of the prepared MoSe_2 thin film shown in Fig. 9, which exhibits positive nonlinear refractive coefficient and the self-focusing behavior of the prepared thin films. The symmetrical nature of the curve was caused by thermally induced nonlinear refractive processes due to employing a CW laser

in experimental setup as a light source. Fig. 9a illustrates the experimental data of pure closed-aperture by fitting with theory. Fig. 9b depicts that with taking into account the error bar by repeating the performing of the experiment for five times.

Due to these thermal effects, the sample behaves as an optical lens (self-focusing effect), leading to an overestimation of nonlinear parameters obtained by the Z-scan method [31]. The nonlinear refractive index is obtained by the following equation [7]:

$$\Delta T_{p-v} = 0.406(1 - s)^{0.25} \left(\frac{2\pi}{\lambda}\right) n_2 I_0 L_{eff} \quad (8)$$

Herein, S denotes the linear transmittance of the aperture found to be 0.36 and λ refers to the wavelength of laser light [38]. The values of



Table 3. Optical parameters of prepared thin films of nanosheets calculated via the Z-scan approach.

Sample	$\alpha_0 (cm^{-1})$	$L_{eff} (\mu m)$	ΔT_{p-v}	$\Delta \varphi$	$n_2 \times 10^{-5} (cm^2/W)$	$\beta \times 10^{-2} (cm/W)$
S1	6.5	19.98	0.0687	0.189	5.28	7.32
S2	8.4	39.99	0.0646	0.178	2.48	5.56
S3	10.3	59.98	0.057	0.157	1.46	4.35

nonlinear coefficients for prepared thin films have been tabulated also in Table 3.

Measured data via Z-scan was numerically fitted using Sheik Bahae's theory to evaluate third-order NLO parameters [9]. Our work demonstrates the significant dependence of both nonlinear refraction and absorption on the thickness of the 2D layers. As thickness of the prepared MoSe₂ thin film increases, the magnitude of n_2 and β decreases.

Since the thermal agitations of particles lead to the change in the local temperature, as, the samples were illuminated by CW Nd : YAG laser and hence, the thermally induced optical nonlinearity predominates over electronic nonlinearity. Therefore, the optical nonlinearity is found to be higher for lower thickness of the MoSe₂ thin film [32].

The same behaviour has obtained for Cu/glass thin films deposited through Thermal Evaporation (TE) and Pulsed Laser Deposition (PLD) techniques [8]. Also, D. Pamu et al. determined that The third order NLO properties of of Bi0.5Na0.5TiO3 thin films were estimated by Z-scan technique employing CW He : Ne laser and the lower thickness of thin film exhibited the strongest nonlinear refractive index ($n_2=4.62 \times 10^{-6} cm^2/W$) and nonlinear absorption coefficient ($\beta = 0.796 cm/W$)[39].

The high dependence of the NLO response on the film thickness is attributed to the topological insulator behavior of the thin film layers. Even slight modifications of the optimal thicknesses can result to a significant loss of the NLO performances [40].

CONCLUSION

A crystalline quality analysis is presented in this study using SEM, TEM, and XRD to determine the crystalline quality of large-area nanosheets. SEM and TEM images confirmed the formation of MoSe₂ nanosheets. It was determined from

the XRD patterns that the nanosheets were hexagonal (a= 3.08 Å, c= 13.72 Å). The structural parameters of MoSe₂ nanosheets are discussed in detail. By employing the Z-scan analysis, the nonlinear absorption index, β and nonlinear refractive index, n_2 of were obtained for all prepared thin films in order of $10^{-2} (cm/W)$, and $10^{-5} (cm^2/W)$ respectively. By using the CW laser regime, the thin film exhibits saturable absorption (SA) and self-focusing properties as a result of thermal nonlinearity and the signs of the n_2 and β were positive. Significant NLO properties have been found, which are highly dependent on the film thickness. The values of nonlinear coefficients of the prepared MoSe₂ thin film decreased with increasing film thickness. We believe that these findings will trigger further research in the field of the optical nonlinearities of 2D photonic materials.

CONFLICTS OF INTEREST

The authors do not have any conflicts of interest.

REFERENCES

- 1 Abutalib M. M., Shkir M., Yahia I. S., AlFaify S., El-Naggar A. M., Ganesh V., (2016), Thickness dependent optical dispersion and nonlinear optical properties of nanocrystalline fluorescein dye thin films for optoelectronic applications. *Optik*. 127: 6601-6609. <https://doi.org/10.1016/j.ijleo.2016.04.136>
- 2 Liu W., Liu M., Han H., Fang S., Teng H., Lei M., Wei Z., (2018), Nonlinear optical properties of WSe2 and MoSe2 films and their applications in passively Q-switched erbium doped fiber lasers. *Photon. Res.* 6: 15-21. <https://doi.org/10.1364/PRJ.6.000C15>
- 3 Wang G., Liang G., Baker-Murray A. A., Wang K., Wang J. J., Zhang X., Bennett D., Luo J. T., Wang J., Fan P., Blau W. J., (2018), Nonlinear optical performance of few-layer molybdenum diselenide as a slow-saturable absorber. *Photon. Res.* 6: 674-680. <https://doi.org/10.1364/PRJ.6.000674>
- 4 Wang G., Baker-Murray A. A., Blau W. J., (2019), Saturable absorption in 2D nanomaterials and related photonic devices. *Laser Photonics Rev.* 13: 1800282. <https://doi.org/10.1002/lpor.201800282>
- 5 Wang K., Wang J., Fan J., Lotya M., O'Neill A., Fox



- D., Feng Y., Zhang X., Jiang B., Zhao Q., (2013), Ultrafast saturable absorption of two-dimensional MoS₂ nanosheets. *ACS Nano*. 7: 9260-9267. <https://doi.org/10.1021/nn403886t>
- 6 Dehghani Z., Ostovari F., Nadafan M., (2022), Investigation of the structural, dielectric, and optical properties of MoSe₂ nanosheets. *J. Appl. Phys.* 131: 213101. <https://doi.org/10.1063/5.0088016>
- 7 Kaur R., Singh K. P., Tripathi S. K., (2020), Study of linear and non-linear optical responses of MoSe₂-PMMA nanocomposites. *J. Mater. Sci.* 31: 19974-19988. <https://doi.org/10.1007/s10854-020-04520-2>
- 8 Etmian M., Hosseini N. S., Ajamgard N., Koohian A., Ranjbar M., (2019), The effect of thin film thickness on thermal nonlinear optical properties and surface morphology of Cu nanostructure thin films. *Optik*. 199: 163517. <https://doi.org/10.1016/j.jileo.2019.163517>
- 9 Sheik-bahae M., Said A. A., Van Stryland E. W., (1989), High-sensitivity, single-beam n₂ measurements. *Opt. Lett.* 14: 955-957. <https://doi.org/10.1364/OL.14.000955>
- 10 Li H., Xia H., Lan C., Li C., Zhang X., Li J., Liu Y., (2015), Passively Q-switched erbium-doped fiber laser based on few-layer MoS₂ saturable absorber. *IEEE Photonics Technol. Lett.* 27: 69-72. <https://doi.org/10.1109/LPT.2014.2361899>
- 11 Khazaeinezhad R., Kassani S. H., Nazari T., Jeong H., Kim J., Choi K., Lee J. U., Kim J. H., Cheong H., Yeom D. I., (2015), Saturable optical absorption in MoS₂ nano-sheet optically deposited on the optical fiber facet. *Opt. Commun.* 335: 224 -230. <https://doi.org/10.1016/j.optcom.2014.09.038>
- 12 Xia H., Li H., Lan C., Li C., Zhang X., Zhang S., Liu Y., (2014), Ultrafast erbium-doped fiber laser mode-locked by a CVD-grown molybdenum disulfide (MoS₂) saturable absorber. *Opt. Express*. 22: 17341-17348. <https://doi.org/10.1364/OE.22.017341>
- 13 Wang S., Yu H., Zhang H., Wang A., Zhao M., Chen Y., Mei L., Wang J., (2014), Broadband few-layer MoS₂ saturable absorbers. *Adv. Mater.* 26: 3538 -3544. <https://doi.org/10.1002/adma.201306322>
- 14 Xu B., Cheng Y., Wang Y., Huang Y., Peng J., Luo Z., Xu H., Cai Z., Weng J., Moncorge R., (2014), Passively Q-switched Nd:YAlO₃ nanosecond laser using MoS₂ as saturable absorber. *Opt. Express*. 22: 28934 -28940. <https://doi.org/10.1364/OE.22.028934>
- 15 Kong L., Xie G., Yuan P., Qian L., Wang S., Yu H., Zhang H., (2015), Passive Q-switching and Q-switched mode-locking operations of 2 μm Tm:CLNGG laser with MoS₂ saturable absorber mirror. *Photonics Res.* 3: A47 -A50. <https://doi.org/10.1364/PRJ.3.000A47>
- 16 Du J., Wang Q., Jiang G., Xu C., Zhao C., Xiang Y., Chen Y., Wen S., Zhang H., (2014), Ytterbium-doped fiber laser passively mode locked by few-layer Molybdenum Disulfide (MoS₂) saturable absorber functioned with evanescent field interaction. *Sci. Rep.* 4: 6346-6351. <https://doi.org/10.1038/srep06346>
- 17 Zhang H., Lu S., Zheng J., Du J., Wen S., Tang D., Loh K., (2014), Molybdenum disulfide (MoS₂) as a broadband saturable absorber for ultrafast photonics. *Opt. Express*. 22: 7249 -7260. <https://doi.org/10.1364/OE.22.007249>
- 18 Liu M., Qi Y. L., Liu H., Luo A.P., Luo Z.C., Xu W.C., Chu-Jun Zhao C.J., Zhang H., (2014), Microfiber-based few-layer MoS₂ saturable absorber for 2.5 GHz passively harmonic mode-locked fiber laser. *Opt. Express*. 22: 22841 -22846. <https://doi.org/10.1364/OE.22.022841>
- 19 Ferrando A., Martínez Pastor J. P., Suárez I., (2018), Toward metal halide perovskite nonlinear photonics. *J. Phys. Chem. Lett.* 9: 5612-5623. <https://doi.org/10.1021/acs.jpcclett.8b01967>
- 20 Dehghani Z., Nadafan M., Mohammadzadeh Shamloo M. B., Shadrokh Z., Gholipour S., Rajabi Manshadi M. H., Darbari S., Abdi Y., (2022), Investigation of dielectric, linear, and nonlinear optical properties of synthesized 2D Ruddlesden-Popper-type halide perovskite. *Opt. Laser Technol.* 155: 108352. <https://doi.org/10.1016/j.optlastec.2022.108352>
- 21 Khazaeizhad R., Kassani S. H., Jeong H., Yeom D. I., Oh K., (2014), Mode-locking of Er-doped fiber laser using a multilayer MoS₂ thin film as a saturable absorber in both anomalous and normal dispersion regimes. *Opt. Express*. 22: 23732 -23742. <https://doi.org/10.1364/OE.22.023732>
- 22 Saminathan R., Hadidi H., Tharwan M., Alnujaie A., Khamaj J. A., Venugopal G., (2022), Raman spectroscopy-assisted characterization of nanoform MoS₂ thin film Transistor, overview. *Scanning*. 2022: Article ID 3255615. <https://doi.org/10.1155/2022/3255615>
- 23 Zhang D., Wen C., Mcclimon J. B., Masih Das P., Zhang Q., Leone A. G., Srinivas V., Mandyam S., Drndić M., Charlie Johnson A. T., Zhao M. Q., (2021), Rapid growth of monolayer MoSe₂ films for large-area electronics. *Adv. Electron. Mater.* 7: 2001219. <https://doi.org/10.1002/aeml.202001219>
- 24 Hsu C., Frisenda R., Schmidt R., Arora A., Vasconcellos S. M., Bratschitsch R., Zant H. S. J., Castellanos-Gomez A., (2019), Thickness-dependent refractive index of 1L, 2L, and 3L MoS₂, MoSe₂, WS₂, and WSe₂. *Adv. Opt. Mater.* 7: 1900239. <https://doi.org/10.1002/adom.201900239>
- 25 Zhang J., Wu M., Liu T., Kang W., Xu J., (2017), Hierarchical nanotubes constructed from interlayer-expanded MoSe₂ nanosheets as highly durable electrodes for sodium storage. *J. Mater. Chem. A* 5: 24859-24866. <https://doi.org/10.1039/C7TA08538A>
- 26 Ghritlahre V., Kumari J., Agarwal P., (2017), Synthesis and study of molybdenum diselenide (MoSe₂) by Solvo-thermal method, AIP Conference Proceedings. 1953: 050048-1-050048-4. <https://doi.org/10.1063/1.5032703>
- 27 Ravinder G., Sreelatha C. J., Ganesh V., Shkir M., Anis M., Rao P. C., (2019), Thickness-dependent structural, spectral, linear, nonlinear and z-scan optical studies of V2O₅ thin films prepared by a low-cost sol-gel spin coating technique. *Mater. Res. Express*. 6: 096403. <https://doi.org/10.1088/2053-1591/ab2992>
- 28 Kamaraj C., Pasupathi G., (2022), Growth and characterization of a semi-organic nonlinear optical single crystal: Sarcosine barium chloride. *J. Mater. Sci. Mater.* 33: 3501-3513. <https://doi.org/10.1007/s10854-021-07542-6>
- 29 Wu Z., Lu Y., Huang J., Peng J., He C., (2022), Third-order optical nonlinearity measurements and optical limiting experiment in Tm: YAG crystal. *Appl. Opt.* 61: 392-397. <https://doi.org/10.1364/AO.445128>
- 30 Habibi M., Davoodianidalik M., (2018), High Power laser systems, Chapter 10: Self-Focusing



- of High-Power Laser Beam through Plasma. <https://doi.org/10.5772/intechopen.75036>
- 31 Felip S. V., (2011), Nitride-based semiconductor nanostructures for applications in optical communications at 1.5 μm , PhD thesis, Departamento de Electrónica, Universidad de Alcalá.
- 32 Egwunyenga J., Onuabuchi V., Okoli L., Nwankwo E., (2021), Effect of SILAR cycles on the thickness, structural, optical properties of cobalt selenide thin films. *Int. Res. J. Multidiscip. Technovation*. 3: 1-9. <https://doi.org/10.34256/irjmt2141>
- 33 Koneva N. A., Solov'eva Y. V., Starenchenko V. A., Kozlov E. V., (2009), Parameters of dislocation structure and work hardening of Ni₃Ge. *Mater. Res. Soc.* 842: 1-6. <https://doi.org/10.1557/PROC-842-S5.25>
- 34 Jigi G. M., Abza T., Girma A., (2021), Synthesis and characterization of aluminum doped zinc sulfide (Al : ZnS) thin films by chemical bath deposition techniques. *J. Appl. Biotechnol. Bioeng.* 8: 55-58. <https://doi.org/10.15406/jabb.2021.08.00252>
- 35 Dehghani Z., Ostovari F., Sharifi S., (2023), A comparison of the crystal structure and optical properties of reduced graphene oxide and aminated graphene nanosheets for optoelectronic device applications. *Optik*. 274: 170551. <https://doi.org/10.1016/j.ijleo.2023.170551>
- 36 Li J., Li H., Hao J., (2022), Fullerene superlattices containing charge transfer complexes for enhanced nonlinear optical performance. *Nanoscale*. 14: 2344-2351. <https://doi.org/10.1039/D1NR06748F>
- 37 Nadafan M., Dehghani Z., Shadrokh Z., Abdi Y., (2023), A remarkable third-order nonlinear optical behavior of single-crystal bromide organic-inorganic lead halide perovskite. *Opt. Laser Technol.* 160: 109055. <https://doi.org/10.1016/j.optlastec.2022.109055>
- 38 Gundogdu Y., Sarilmaz A., Gencer A., Ozel F., Surucu G., Kilic H. S., Ersoz M., (2022), Copper-based thiospinel quantum dots as potential candidates for nonlinear optical applications. *Opt. Laser Technol.* 148: 107752. <https://doi.org/10.1016/j.optlastec.2021.107752>
- 39 Pattipaka S., Joseph A., Bharti G. P., Raju K. C. J., Khare A., Pamu D., (2019), Thickness-dependent microwave dielectric and nonlinear optical properties of Bi_{0.5}Na_{0.5}TiO₃ thin films, *Appl. Surf. Sci.* 488: 391-403. <https://doi.org/10.1016/j.apsusc.2019.05.264>
- 40 Verrone R. N., Moisset C., Lemarchand F., Campos A., Cabié M., Perrin-Pellegrino C., Lumeau J., Natoli J. Y., Iliopoulos K., (2020), Thickness-dependent optical nonlinearities of nanometer-thick Sb₂Te₃ thin films: Implications for mode-locking and super-resolved direct laser writing. *ACS Appl. Nano Mater.* 3: 7963-7972. <https://doi.org/10.1021/acsnm.0c01445>